The Astrophysical Journal, 663:103–117, 2007 July 1

THE INTRINSICALLY X-RAY WEAK QUASAR PHL 1811. I. X-RAY OBSERVATIONS AND SPECTRAL ENERGY DISTRIBUTION[1]

Karen M. Leighly
Homer L. Dodge Department of Physics and Astronomy, University of Oklahoma, 440 West Brooks Street, Norman, OK 73019; leighly@nhn.ou.edu

Jules P. Halpern
Department of Astronomy, Columbia University, 550 West 120th Street, New York, NY 10027-6601

Edward B. Jenkins
Princeton University Observatory, Princeton, NJ 08544-1001

Dirk Grupe
Department of Astronomy and Astrophysics, Pennsylvania State University, 525 Davey Lab, University Park, PA 16802

and

Jiehae Choi[2] and Kimberly B. Prescott
Homer L. Dodge Department of Physics and Astronomy, University of Oklahoma, 440 West Brooks Street, Norman, OK 73019
Received 2006 March 24; accepted 2006 October 16

ABSTRACT

This is the first of two papers reporting observations and analysis of the unusually bright ($m_b = 14.4$), luminous ($M_B = -25.5$), nearby ($z = 0.192$) narrow-line quasar PHL 1811, focusing on the X-ray properties and the spectral energy distribution. Two *Chandra* observations reveal a weak X-ray source with a steep spectrum. Variability by a factor of 4 between the two observations separated by 12 days suggests that the X-rays are not scattered emission. The *XMM-Newton* spectra are modeled in the 0.3–5 keV band by a steep power law with $\Gamma = 2.3 \pm 0.1$, and the upper limit on intrinsic absorption is 8.7×10^{20} cm^{-2}. The spectral slopes are consistent with power-law indices commonly observed in NLS1s, and it appears that we observe the central engine X-rays directly. Including two recent *Swift* ToO snapshots, a factor of $\sim$5 variability was observed among the five X-ray observations reported here. In contrast, the UV photometry obtained by the *XMM-Newton* OM and *Swift* UVOT, and the *HST* spectrum reveal no significant UV variability. The α_{ox} inferred from the *Chandra* and contemporaneous *HST* spectrum is -2.3 ± 0.1, significantly steeper than observed from other quasars of the same optical luminosity. The steep, canonical X-ray spectra, lack of absorption, and significant X-ray variability lead us to conclude that PHL 1811 is intrinsically X-ray weak. We also discuss an accretion disk model and the host galaxy of PHL 1811.

Subject headings: quasars: emission lines — quasars: individual (PHL 1811) — X-rays: galaxies

1. INTRODUCTION

The standard model for active galactic nuclei (AGNs) and quasi-stellar objects (QSOs) proposes that the broadband optical and UV continuum originates in an accretion disk. The X-ray emission is a separate component, produced in a corona located in the vicinity of the disk, that creates the X-rays by inverse Compton scattering the disk photons. This broadband continuum is then thought to illuminate the gas that forms the broad-line region, causing it to emit lines via photoionization.

Despite the commonality of the origin of the optical through X-ray continuum emission and emission lines, there are theoretical reasons that the spectra should vary among individual objects. The origin of differences may be extrinsic; for example, the brightness and, to some extent, the shape of the continuum spectrum of the accretion disk should vary with viewing angle (e.g., Laor & Netzer 1989). The origin may also be intrinsic. Even for very simple disk models, in which the spectrum is constructed from a sum of annuli locally emitting as blackbodies, the continuum spectrum from the accretion disk should depend on the black hole mass and accretion rate (e.g., Frank et al. 1992). More sophisticated accretion disk models that include a range of physical processes expected to be important also predict a range of shapes (e.g., Kato et al. 1998). Another complication is that the type of accretion disk present is predicted to depend on the accretion rate relative to the Eddington value (e.g., Chen et al. 1995), and the type of accretion disk can be different at different radii (e.g., Svensson & Zdziarski 1994). The X-ray emitting corona adds another dimension of complication, as its origin and geometry are not very well understood. Thus, in principle, the coronal emission may or may not be important depending on how much of the accretion energy is funneled to it, and indeed, we see evidence for a range of coronal activity in X-ray novae (e.g., Kubota & Done 2004).

In addition to the theoretical expectation of a range of predicted spectral energy distributions among AGNs, there is observational evidence that such a range exists. In a study of the multiwavelength properties of an X-ray selected heterogeneous sample of quasars, Elvis et al. (1994) observed a wide range of spectral energy distributions (SEDs). Wilkes et al. (1994) and more recently Bechtold et al. (2003), Strateva et al. (2005), and Steffen et al. (2006) found that α_{ox}, the point-to-point slope between the

[1] Based on observations obtained with *XMM-Newton*, an ESA science mission with instruments and contributions directly funded by ESA Member States and NASA.

[2] Current address: Department of Astronomy, New Mexico State University, P.O. Box 30001, MSC 4500, Las Cruces, NM 88003-8001.

TABLE 1
Observing Log

Observatory and Instrument	Date	Exposure (s)	Bandpass or Effective Wavelength	Extraction Radius (arcsec)
Chandra ACIS-S3	2001 Dec 5	9377	0.3–10 keV	3.94
Chandra ACIS-S3	2001 Dec 17	9839	0.3–10 keV	3.94
XMM-Newton PN	2004 Nov 1	27472	0.3–12 keV	27
XMM-Newton MOS1	...	32126	0.5–10 keV	23
XMM-Newton MOS2	...	32164	0.5–10 keV	23
XMM-Newton OM (UVM2)	...	25800	2310 Å	12
Swift XRT (PC mode)	2005 Oct 22	2462	0.3–10 keV	23.4
Swift UVOT (UVW1)	...	787	2600 Å	12
Swift UVOT (UVM2)	...	844	2200 Å	12
Swift UVOT (UVW2)	...	844	1930 Å	12
Swift XRT (PC mode)	2006 May 12	1600	0.3–10 keV	23.4
Swift UVOT (*V*)	...	130	5460 Å	6
Swift UVOT (*B*)	...	130	4350 Å	6
Swift UVOT (*U*)	...	130	3450 Å	6
Swift UVOT (UVW1)	...	259	2600 Å	12
Swift UVOT (UVM2)	...	372	2200 Å	12
Swift UVOT (UVW2)	...	526	1930 Å	12
MDM McGraw-Hill 1.3 + *I* + Templeton	2004 Oct 14–16	5, 3, 1[a]	8050 Å	5.8–10.0
MDM McGraw-Hill 1.3 + *V* + Templeton	...	5, 9, 5[a]	5380 Å	5.7–10.1
MDM McGraw-Hill 1.3 + *B* + Templeton	...	5, 5, 2[a]	4350 Å	6.2–10.0
MDM McGraw-Hill 1.3 + *U* + Templeton	...	5, 5, 2[a]	3640 Å	6.8–10.2

[a] Number of frames on each of the three days.

2500 Å and 2 keV, is inversely correlated with the UV luminosity. In many objects, the large range of spectral energy distributions can be accounted for by extrinsic effects such as reddening and absorption (e.g., Brandt et al. 2000). However, these extrinsic effects certainly cannot account for the range of SEDs in *all* objects.

PHL 1811 is a nearby ($z = 0.192$), luminous ($M_B = -25.5$) narrow-line quasar. PHL 1811 was first cataloged as a blue object in the Palomar-Haro-Luyten plate survey (Haro & Luyten 1962). It was then rediscovered in the optical follow-up of the VLA Faint Images of the Radio Sky at Twenty cm (FIRST) survey (White et al. 1997; Becker et al. 1995). It is extremely bright ($B = 14.4$, $R = 14.1$); it is the second brightest quasar at $z > 0.1$ after 3C 273. Because it is so bright, it is a very good background source for studies of the intergalactic and interstellar medium; furthermore, a *FUSE* observation found its spectrum to have a rare Lyman limit system that has been studied by Jenkins et al. (2003, 2005). It was odd, however, that such a bright quasar was not detected in the *ROSAT* All Sky Survey (RASS). In comparison with other quasars of its luminosity, the expected RASS count rate is about 0.5 s^{-1}; we placed an upper limit of 1.3×10^{-2} counts s^{-1} (Leighly et al. 2001). A pointed *BeppoSAX* observation detected the object, but it was still anomalously weak. Too few photons were obtained in the *BeppoSAX* observation to unambiguously determine the cause of the X-ray weakness; Leighly et al. (2001) speculated that either it is intrinsically X-ray weak, or it is a nearby broad absorption line quasar and the X-ray emission is absorbed, or it is highly variable, and we caught it both times in a low state.

In this paper and the companion paper (Leighly et al. 2007, hereafter Paper II) we report the results of several UV and X-ray observations of PHL 1811 designed to explore the origin and consequences of the X-ray weakness of this object. First, coordinated *Chandra* and *HST* observations were made in 2001. In 2004, an *XMM-Newton* observation was made, and most recently, PHL 1811 was the target of two *Swift* Target of Opportunity observations. In § 2 we describe the results and analysis of the *Chandra*, *XMM-Newton*, and *Swift* observations, as well as the results of a 3 day optical photometry run at MDM Observatory. We also compare the *XMM-Newton* spectrum of PHL 1811 with those from other narrow-line Seyfert 1 galaxies (NLS1s). In § 3 we comment on the long timescale X-ray and UV variability. We present an updated spectral energy distribution in § 4. In § 5, we discuss the nature of the intrinsic X-ray weakness and present an accretion disk model for PHL 1811. We also comment on the apparent spiral host galaxy discovered in the image presented by Jenkins et al. (2005). We summarize our findings in § 6. Paper II describes the *HST* and ground-based optical and UV observations and presents Cloudy models that explore the unusual emission-line properties. Some of the results were presented previously in Leighly et al. (2004), Choi et al. (2005), and Prescott (2006). We assume a flat universe with $H_0 = 70$ km s^{-1} Mpc^{-1} and $\Omega_{vac} = 0.73$ unless otherwise specified.

2. OBSERVATIONS AND ANALYSIS

2.1. *Chandra* Observations and Analysis

The *Chandra* observations were made in imaging spectroscopy mode with the image of PHL 1811 placed on the ACIS-S3 detector. The observing log is given in Table 1. We verify that the position of the X-ray source is consistent with that of the quasar (Fig. 1).

The level 2 event files were recreated using the standard procedure. The small correction for the time-dependent gain was applied using the `corr_tgain` program, and the correction for the time-dependent ancillary matrix was made using the IDL program `acisabs.pro`.[3] The total count rates observed within a circular region 3.94″ in radius were 9.7×10^{-3} and 4.0×10^{-2} counts s^{-1} from the first and second observations, respectively. These rates are low enough that pileup is negligible. Between 0.3 and 9.8 keV,

[3] See http://www.astro.psu.edu/users/chartas/xcontdir/xcont.html.

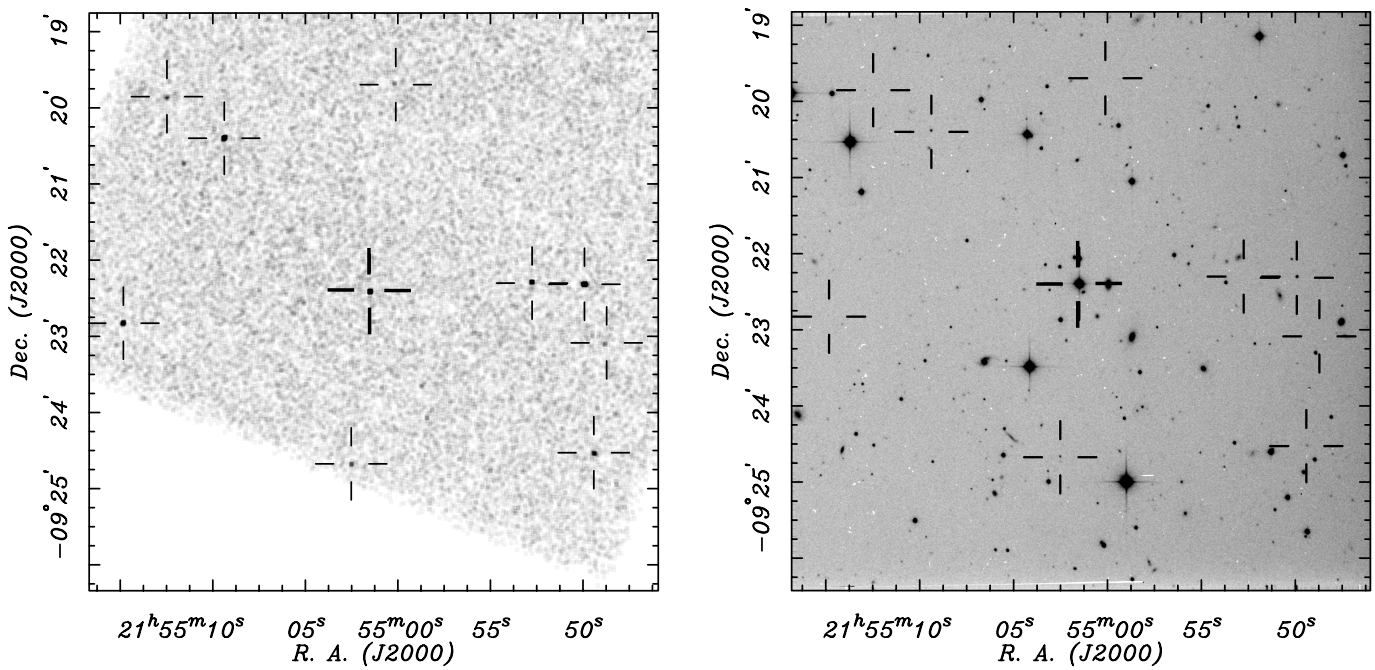

FIG. 1.—*Chandra* image (*left*) and MDM optical *R*-band image (*right*) showing that the X-ray source is securely identified as PHL 1811.

a total of 81 and 374 photons were obtained. Based on the background collected from source-free areas of the chips, we expect 1 and 3 of these photons to originate in the background. Thus, we can conclude that we observe a significant change in flux in the object by about a factor of 4 between the two observations separated by 12 days.

A sufficient number of photons were collected in the second observation to look for short timescale variability. We used the Bayesian Blocks program available in the ISIS software[4] but did not find any indication of variability during the observation at significance levels greater than about 1 σ. We also tried binning the light curve with 100 s bins and then grouping together by hand points that appeared low or high. The χ^2 for a constant model was 13.5 for 6 degrees of freedom (dof), indicating that variability was marginally detected with confidence of 96.4%, although the probability that this variability is significant may be lower because the results are biased by preselecting the bin sizes. Note that the $\Delta\chi^2 = 6.63$ uncertainty on the fitted constant model is 14%, indicating that we are only sensitive to variations larger than this value at the 99% confidence level. Such high-amplitude variations are rare but not unprecedented in luminous NLS1s (e.g., Leighly 1999a).

The spectra were accumulated and grouped so there were ~20 photons in each bin. We first fitted each spectrum between 0.3 and 5 keV separately with a power law and fixed Galactic column of 3.76×10^{20} cm^{-2}, obtained using the HEASARC $n_{\rm H}$ tool.[5] We note that the Galactic Lyα line in the medium-resolution UV spectrum of PHL 1811 (Jenkins et al. 2005) is consistent with this value of $N_{\rm H}$. This model fits both spectra well, yielding photon indices of $2.01^{+0.37}_{-0.36}$ and $2.58^{+0.19}_{-0.18}$ for the first and second *Chandra* observations, respectively. These photon indices are consistent with those observed from NLS1s by *ASCA* (Leighly 1999b). Note that the *ASCA* photon indices were taken from models spanning the ~0.5–10 keV band that include a soft excess, warm absorber, and iron line as necessary. Thus, the *Chandra* spectra from PHL 1811, fitted over 0.3–5.0 keV (0.36–5.96 rest frame), are consistent with the hard X-ray power law found in *ASCA* spectra of NLS1s.

The best-fitting photon index is steeper for the second, brighter observation, suggesting that shape of the spectrum has changed between the two observations. However, the uncertainties indicate that the difference is not statistically significant. Fitting the spectra simultaneously and using the *F*-test shows that the improvement in the fit represented by a change in the photon index is significant at only the 68% confidence level. Figure 2 shows these model fits.

In order to see whether there is any evidence for intrinsic absorption, we next fit the spectrum from the second observation with a model consisting of a power law, absorption fixed at the Galactic value, and absorption in the rest frame of the quasar. We find no improvement in the fit, and the best-fitting value of additional intrinsic absorption is zero. The $\Delta\chi^2 = 2.71$ upper limit on the intrinsic absorption column is 1.8×10^{20} cm^{-2}. The upper limit is rather low despite the poor photon statistics in the spectrum because the spectrum is convex (Fig. 2).

The convex residuals of the power-law fit to the second observation suggest the presence of a soft excess (Fig. 2). Soft excess components are common in the spectra of NLS1s and in the case of poor statistics can be fitted adequately by a blackbody model (e.g., Leighly 1999b). We add a blackbody component to the power-law model for the second spectrum and find that the fit improves by $\Delta\chi^2 = 4.9$, and the residuals are flat (Table 2). However, the improvement in the fit is not statistically significant; the *F*-test shows that the improvement in fit is significant at only the 71% confidence level. Thus, we cannot conclude that a soft excess is present, because of the poor statistics.

The power-law index for the power law plus blackbody fit to the second observation is flatter than for the power law alone (2.22 ± 0.34 vs. $2.58^{+0.19}_{-0.18}$) and is now completely consistent with that of the first observation ($2.01^{+0.37}_{-0.36}$). This suggests that the spectral variability originates as an emergence of the blackbody component when the object is brighter. To investigate this

[4] See http://space.mit.edu/CXC/analysis/SITAR/index.html.
[5] Available at http://heasarc.gsfc.nasa.gov/cgi-bin/Tools/w3nh/w3nh.pl.

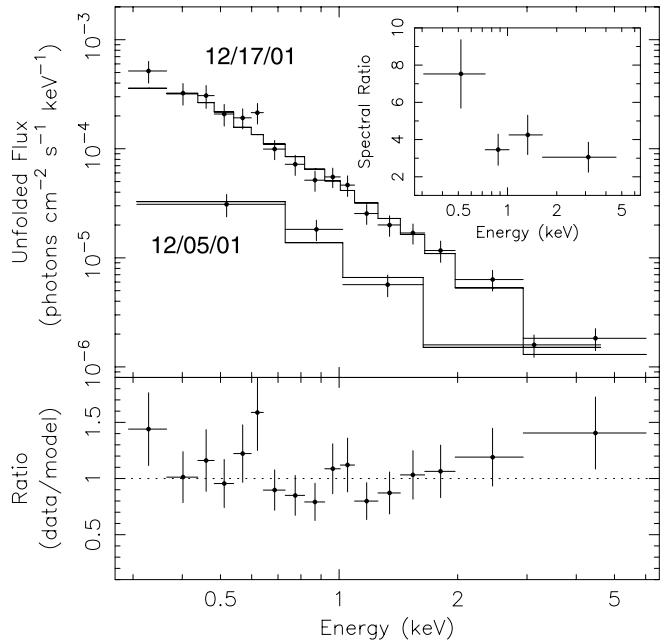

FIG. 2.—*Top*: Unfolded best-fitting power-law models for the spectra from the two *Chandra* observations. *Bottom*: Residuals from a power-law model fit to the spectrum from the second observation, with a convex shape suggesting the presence of a soft excess. *Inset*: Ratio of the second spectrum to the first spectrum showing that the spectral variability is predominately confined to the softest energies, suggesting the emergence of a soft excess component when the object is bright.

possibility, we fit both spectra simultaneously with a power law plus blackbody model, fixing the normalization of the blackbody for the first observation to zero. The model fits the data adequately ($\chi^2_\nu = 0.67$ for 16 dof). The jointly fitted photon index is 2.12 ± 0.25, and for this parameterization, the normalizations of the power law differ by a factor of 3.5.

Spectral ratios provide a complementary and model-independent approach to the question of spectral variability. We rebin the spectrum from the second observation to the binning of the first spectrum and take their ratio (Fig. 2, *inset*). This shows that the spectral variability is predominately in the softest band, supporting our hypothesis that a variable soft excess is responsible for the spectral variability. In this case, the variability of the power-law component is a factor of 3.5. The χ^2 for a constant-ratio model is 3.8 for 3 degrees of freedom, which significant at the 71% confidence level.

To summarize the results of the *Chandra* observations, we find conclusive evidence for factor of $\sim$4 variability between the two observations separated by 12 days. Detailed analysis is hampered by poor statistics; however, we find marginal evidence ($2\,\sigma$) for variability on timescales of thousands of seconds in the second observation, when the object was brighter. Spectral fitting reveals a steep spectrum with no evidence for intrinsic absorption, and marginal evidence for spectral variability between the observations, with the spectrum becoming steeper when the object is brighter. The spectral fitting and the ratio of the spectra suggest that the spectral variability is caused by the emergence of a soft excess component when the object is bright. The measured spectral indices range between 2.0 and 2.6, depending on the model. They are consistent with the photon indices measured in *ASCA* observations of NLS1s (Leighly 1999b). This fact suggests that we see the intrinsic X-ray emission from the central engine and

TABLE 2
Chandra SPECTRAL FITTING RESULTS

Parameter	2001 Dec 5	2001 Dec 17
Power-Law Model, Spectra Fitted Separately		
Photon index	$2.01^{+0.37}_{-0.36}$	$2.58^{+0.19}_{-0.18}$
Normalization[a]	$(1.17 \pm 0.02) \times 10^{-5}$	$(5.10 \pm 0.45) \times 10^{-5}$
Flux (0.3–5 keV; erg cm^{-2} s^{-1})	5.2×10^{-14}	2.3×10^{-13}
Luminosity (0.3–5 keV; erg s^{-1})	5.6×10^{42}	2.4×10^{43}
χ^2/dof	1.96/2	13.2/15
Power Law + Blackbody[b]		
Photon index	...	2.22 ± 0.34
Power-law normalization[a]	...	$4.4^{+0.83}_{-1.0} \times 10^{-5}$
Blackbody temperature (keV)	...	$0.096^{+0.040}_{-0.081}$
Blackbody normalization[c]	...	$1.5^{+\infty}_{-1.1} \times 10^{-6}$
χ^2/dof	...	8.36/13
Power Law + Blackbody,[b] Joint Fit		
Photon index	2.12 ± 0.25[d]	2.12 ± 0.25[d]
Power-law normalization[a]	$(1.17 \pm 0.22) \times 10^{-5}$	$4.14^{+0.79}_{-0.84} \times 10^{-5}$
Blackbody temperature (keV)	$0.10^{+0.035}_{-0.042}$[d]	$0.10^{+0.035}_{-0.042}$[d]
Blackbody normalization[c]	0[e]	$1.5^{+2.7}_{-0.82} \times 10^{-6}$
χ^2/dof	10.8/16 [d]	10.8/16[d]

[a] In units of photons keV^{-1} cm^{-2} s^{-1} at 1 keV in the observed frame.
[b] The blackbody temperature is given in the rest frame.
[c] In units of L_{39}/D_{10}^2, where L_{39} is the source luminosity in units of 10^{39} erg s^{-1}, and D_{10} is the distance to the object in units of 10 kpc.
[d] Parameter fitted jointly.
[e] Fixed parameter.

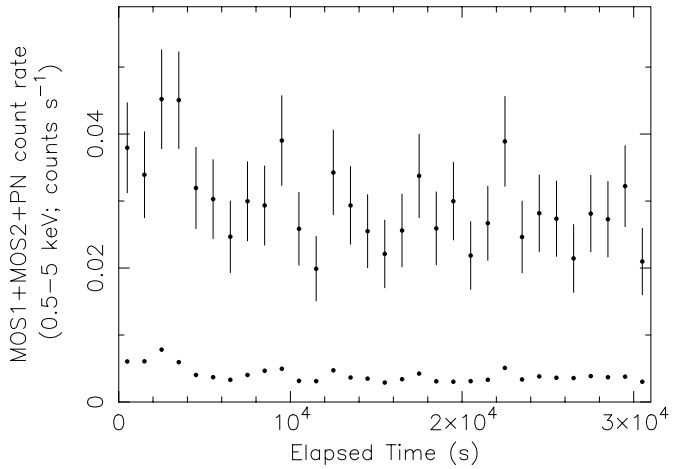

FIG. 3.—*XMM-Newton* background-subtracted light curve composed of the 0.5–5 keV photons from the MOS1, MOS2, and PN detectors. The lower light curve shows the estimated background in the source extraction region. There is no strong evidence for variability over the 31 ks observation.

that the X-rays are powered by inverse Compton scattering of soft photons as in other AGNs.

2.2. *XMM-Newton Observation and Analysis*

PHL 1811 was observed by *XMM-Newton* on 2004 November 1 using the EPIC PN (Strüder et al. 2001) and MOS (Turner et al. 2001) instruments and the Optical Monitor (OM; Mason et al. 2001). The EPIC observations were carried out using the thin filter in PrimeFullWindow mode. The data were reduced using standard selection criteria. The object was observed for 32.1 ks using the MOS detectors and for 27.5 ks using the PN. The details of the observation are given in Table 1.

Background flares are a concern in *XMM-Newton* data analysis, and we observed the background to vary during the observation. For most of the observation, the background was relatively low and stable. However, even at the lowest rate, it appears to be slightly elevated compared with the quiescent rate[6] by a factor of approximately 2.3 for the PN and 1.4 in the MOS1 + MOS2 in both the soft (0.5–2.0 keV) and hard (2.0–10 keV) bands. In addition, for the first 3000 s in the PN detector, and the first 5000 s for the MOS detector, there occurred a small background flare that was higher than the quiescent rate by a factor of 2–3. We extracted and analyzed spectra with and without this flaring period and conclude that the flare is so small that it does not adversely affect the results. Therefore, we analyze the entire exposure.

We extract light curves from the PN and MOS detectors. The target is relatively weak, so we use a source extraction region with a radius corresponding to an encircled energy function of 80%; the radius was 27″ for the PN and 23″ for the MOS1 and MOS2. Background light curves and spectra were extracted from nearby, source-free regions of the detector. The background spectrum is flatter than the source spectrum, and we find that the background contribution to the emission in the extraction aperture is equal to that of the target at ~5 keV. The background dominates at higher energies; therefore, we extract light curves in the 0.5–5 keV band. We use a bin size of 1000 s, which yields an average of ~30 source counts per bin, and the background contributes about 12% of the total counts. The resulting background-subtracted light curve is shown in Figure 3. The mean count rate is $(2.8 \pm 0.17) \times 10^{-3}$ counts s^{-1}. The light curve is statistically consistent with no variability ($\chi^2 = 33.4$ for 30 dof for a constant model). Note that the $\Delta\chi^2 = 6.63$ uncertainty on the fitted constant model is 9%, indicating that we are only sensitive to variations larger than this value at the 99% confidence level. Such high-amplitude variations are rare but not unprecedented in luminous NLS1s (e.g., Leighly 1999a).

[6] See *XMM-Newton* User's Handbook, § 3.3.8 (http://heasarc.gsfc.nasa.gov/docs/xmm/uhb/node38.html).

TABLE 3

XMM-Newton SPECTRAL FITTING RESULTS

Parameter	Measurement
Photon index	$2.28^{+0.12}_{-0.11}$
PN normalization[a,b]	1.16 ± 0.98
MOS1 normalization offset[a]	$1.25^{+0.21}_{-0.19}$
MOS2 normalization offset[a]	$1.32^{+0.22}_{-0.20}$
Flux (0.3–5 keV; erg cm^{-2} s^{-1})	5.1×10^{-14}
Luminosity (0.3–5 keV; erg s^{-1})	5.4×10^{42}
χ^2/dof	74.7/79

[a] The spectral model was $C \exp[N_{\rm H}({\rm Gal})\sigma(E)]\,E^{-\Gamma}$, where all parameters were tied together except for the constant C, which was fixed to 1 for the PN and allowed to vary for the MOS1 and MOS2. Unexpected optical loading plausibly causes the MOS spectra to have a higher normalization; therefore, we quote flux and luminosity values from the PN data only.

[b] In units of photons keV^{-1} cm^{-2} s^{-1} at 1 keV in the observed frame.

The spectra were extracted using the regions described above and grouped so that there were 15 photons per energy bin. We simultaneously fit the PN in the 0.3–5 keV range and MOS in the 0.5–5 keV band. The spectra yield 611, 191, and 204 source photons for the PN, MOS1, and MOS2, respectively. The spectra are fitted very well with a model consisting of a constant, a power law, and a Galactic absorption column described in § 2.1. The results are listed in Table 3, and the model fit is shown in Figure 4. Note that unlike the second *Chandra* observation, the residuals are flat, and there is no evidence for a soft excess component.

The spectra are adequately fitted using a steep power law ($\Gamma = 2.3 \pm 0.1$), typical of that from NLS1s observed by *ASCA* (Leighly 1999b). There is no evidence for additional absorption. We add a neutral absorption component at the redshift of PHL 1811 to the model but find no significant reduction in χ^2. The 90% confidence upper limit ($\Delta\chi^2 = 2.7$) on additional absorption is $N_{\rm H} = 8.7 \times 10^{20}$ cm^{-2}.

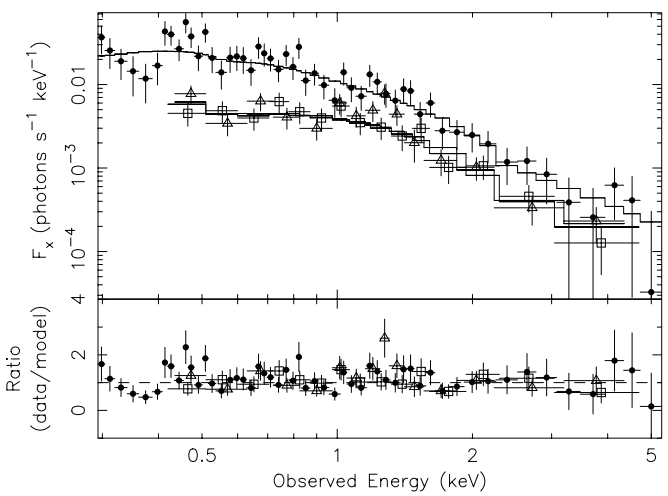

FIG. 4.—*XMM-Newton* MOS1, MOS2, and PN spectra (*open squares, open triangles, and filled circles, respectively*), well fitted using a power law and Galactic absorption. The upper limit on intrinsic X-ray absorption is 8.7×10^{20} cm^{-2}.

The constant in the model is fixed to a value of 1 for the PN spectrum and allowed to be free for the MOS1 and MOS2 spectra. It can be seen in Table 3 that the best-fitting normalizations of MOS1 and MOS2 spectra are 25% and 32% higher than that of the PN, respectively. This difference cannot be explained by residual calibration uncertainty between the *XMM-Newton* EPIC instruments as that is now quite low (Stuhlinger et al. 2006). We analyze the X-ray spectra from another object in the field (located at R.A. $= 21^{h}54^{m}41^{s}$, decl. $= -9^{\circ}26'49''$) that is about 50% brighter than PHL 1811. The normalizations of the EPIC spectra for this object were completely consistent with one another (MOS1 constant: 1.00 ± 0.12; MOS2 constant: $1.00^{+0.13}_{-0.12}$). Another object in the field of view was independently analyzed by another of the authors (D. Grupe) with the same result.

While the small numbers of photons in the PHL 1811 spectra mean that the difference in normalizations among the models for the different EPIC spectra is not statistically significant, there still seems to be a problem with the spectra that needs to be understood. We believe that the problem originates in optical loading. The nominal limit for optical loading using the thin filter is $V \approx 12$ for both the PN and the MOS (Smith 2004; Altieri 2003). PHL 1811 is a fainter optical source ($B = 14.4$, $R = 14.1$); however, it has a very blue spectrum and is a very weak X-ray source, and thus is an unusual object compared with the stellar calibration sources used to determine the loading limits. Another point that supports our contention that optical loading is important is the fact the optical loading in the MOS2 is observed to be about 7% larger than that in the MOS1, possibly due to variations in the filter transmission (Altieri 2003); we also observe a higher normalization for the MOS2 spectrum. However, the degree of contamination by optical photons cannot be very large, because the MOS spectra do not show any observable distortion; a power-law fit to them alone yields an identical photon index with that obtained from the PN. Nevertheless, given the fact that the MOS spectra are possibly contaminated by optical loading, we measure the flux from the PN spectrum, noting that we cannot be sure that this spectrum is uncontaminated by optical loading as well, and may represent an upper limit on the flux for this observation.

PHL 1811 was observed using the Optical Monitor with the UVM2 filter. Ten exposures, each with duration of 2580 s, were made. The SAS task `omichain` was run to reprocess the data. The count rate information was extracted from the `omichain` output. In addition, the count rates were extracted from the images using the IRAF task `phot`. The count rates were then converted to flux using the conversion factor for the UVM2 filter (2.17×10^{-14} erg s^{-1} cm^{-2} Å^{-1} count^{-1}). The results from the two extraction procedures were consistent to within 2%, and therefore hereafter we discuss the results from the `omichain` output.

One of the goals of the OM observation was to look for UV variability. A constant model fit to the light curve yielded $\chi^2 = 16.86$ for 9 degrees of freedom. Thus, a constant model is rejected at the 94.9% confidence level. However, we do not consider this evidence for marginally significant UV variability, because the fluctuations are different for the `omichain` and IRAF-reduced data. The mean flux of the 10 observations was $(2.773 \pm 0.007) \times 10^{-14}$ erg s^{-1} cm^{-2} Å^{-1}.

2.3. *Joint Chandra and XMM-Newton Modeling*

In principle, better constraints on spectral variability can be obtained by jointly fitting the *Chandra* and *XMM-Newton* spectra. We first fit with a power law plus Galactic absorption model, allowing the normalizations to be free among the two *Chandra* spectra and the *XMM-Newton* PN spectrum, but with the photon indices constrained to be equal. The spectra are fitted adequately; the χ^2 is 70.5 for 70 degrees of freedom. The best-fitting photon index is $2.36^{+0.12}_{-0.11}$, again typical of an NLS1 (Leighly 1999b). We notice that the normalization for the spectrum from the first *Chandra* observation is identical to that of the *XMM-Newton* PN spectrum; if we tie these two parameters together, there is no change in χ^2 ($\chi^2 = 70.5$ for 71 degrees of freedom). These two spectra seem to describe the object in the same state (see also § 3), so we leave their parameters tied together throughout the remainder of this section.

Next, we allow the photon index of the second, higher flux *Chandra* observation to be fitted independent of that of the first *Chandra* spectrum and the *XMM-Newton* spectrum. We obtain a somewhat better fit with $\chi^2 = 64.1$ for 70 degrees of freedom. However, the decrease in χ^2 is significant at only the 63% level according to the *F*-test. The resulting photon indices are 2.22 ± 0.14 for the low state (first *Chandra* observation and *XMM-Newton* PN spectrum) and $2.57^{+0.19}_{-0.18}$ for the second, brighter *Chandra* observation. These indices are still within the range of power-law indices observed from NLS1s (Leighly 1999b). In addition, it is often found that the NLS1 spectra soften as when they are brighter (e.g., Fig. 4 of Leighly 1999a); thus, intrinsic softening of the spectrum is a plausible explanation for the marginal spectral variability we observe.

It is possible that the variability results from variable cold absorption. We test this scenario by constraining the photon indices and normalizations to be the same for all three spectra, and including a neutral absorption column in the quasar rest frame in the model, allowing the absorption column to vary. This model gives a very poor fit; the reduced $\chi^2 = 2.57$ for 70 degrees of freedom. Thus, we can reject on statistical grounds the idea that the spectral and flux variability originates solely in variable neutral absorption. Allowing the normalizations to also be free yields a good fit ($\chi^2 = 65.3$ for 69 degrees of freedom), although it is not a significant improvement over the no-absorption model ($\Delta\chi^2 = 5.2$, significant at the 58% confidence level according to the *F*-test). The additional absorption is consistent with zero for the brighter *Chandra* observation with an upper limit of 1.4×10^{20} cm^{-2} and is equal to $5.0^{+3.9}_{-3.6} \times 10^{20}$ cm^{-2} for the fainter *Chandra* observation and the *XMM-Newton* observation. Although this model (variable cold absorption plus variable power-law normalization) fits the spectra well, the scenario seems unlikely because it requires that absorber variability be coordinated with intrinsic flux variability.

2.4. *The X-Ray Spectra of NLS1s: How Does PHL 1811 Compare?*

ASCA observations of NLS1s demonstrate that their spectra can generally be described by a hard power law with an average index of 2.19 ± 0.10 and a soft excess that can be modeled using a blackbody component. The strength of the soft excess varies from object to object, with the objects having the overall steepest spectra also showing the highest amplitude variability (Leighly 1999b).

XMM-Newton, with its large effective area, has revolutionized our understanding of the X-ray spectra of AGNs. Soft excesses are now seen to be relatively common in quasars in general (e.g., Porquet et al. 2004). NLS1 spectra are still found to have soft excess that sometimes can be modeled by a dual Comptonization model, in which soft photons are scattered by Comptonizing media of two different temperatures. Examples of objects with this type of spectrum are Ton S180 (Vaughan et al. 2002) and Mrk 896 (Page et al. 2003). In other cases, the X-ray spectrum is very complex, with a very prominent soft excess and complex absorption features at high energies. These spectra can be modeled using

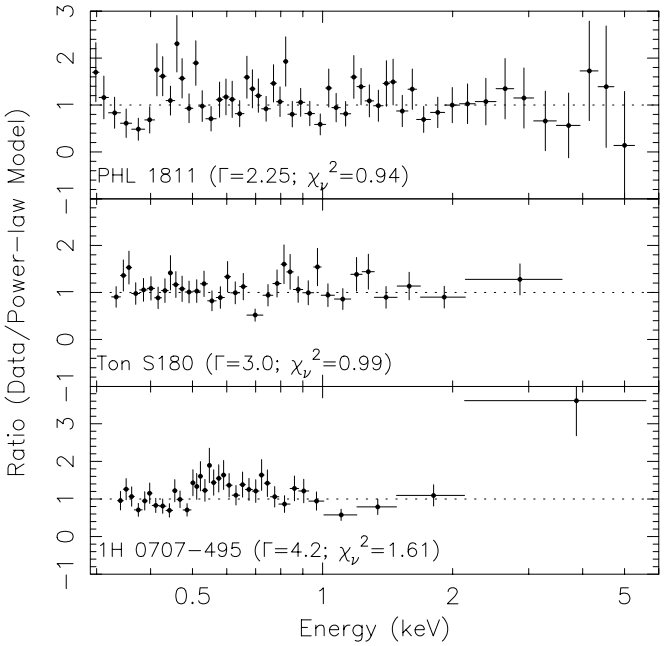

FIG. 5.—Comparison of the *XMM-Newton* PN spectrum from PHL 1811 with spectra from other NLS1s from segments of data short enough for the statistics to be similar. In each panel, the ratio of the data to a power law plus Galactic absorption model is plotted. The resulting power-law index and χ_ν^2 is given in each panel. The top panel shows that PHL 1811 is statistically well described by a power-law model. The photon index is typical of the power-law indices observed from *ASCA* observations of NLS1s (Leighly 1999b). In the middle panel, Ton S180, an NLS1 classified as having a "simple" spectrum by Gallo (2006), is statistically well described by a power law; however, the index is steep, suggesting that a longer exposure would reveal a hard tail (as it does; Vaughan et al. 2002). In the bottom panel, 1H 0707−495, an NLS1 classified as having a "complex" spectrum by Gallo (2006), shows a very steep spectrum and significant residuals, confirming the necessity of a complex model (e.g., Gallo et al. 2004b; Tanaka et al. 2004).

partial covering (e.g., Tanaka et al. 2004) or reflection (Miniutti & Fabian 2004). Examples of this type of object include 1H 0707−495 (Gallo et al. 2004b; Tanaka et al. 2004), IRAS 13224−3809 (Boller et al. 2003), and PHL 1092 (Gallo et al. 2004a). Gallo (2006) split NLS1s into two classes: those with and without significant complex features in their high-energy spectra. He finds that objects with complex high-energy spectra tend to be X-ray weak and proposes that the X-ray weakness is consistent with either attenuation in the partial covering scenario or the focusing X-rays away from our line of sight in the reflection scenario.

How does the *XMM-Newton* spectrum of PHL 1811 compare with those from other NLS1s? It is important to note that the quality of our spectrum is much poorer than those from many *XMM-Newton* observations of NLS1s, such as those mentioned above, due to its low X-ray flux. The PN spectrum has 857 photons between 0.3 and 5 keV in the observed frame, corresponding to 0.36–5.96 keV in the rest frame. Of these, 246 are background, leaving 611 net source photons. This spectrum is adequately modeled with a power law and absorption originating in our Galaxy. The reduced χ^2 is 0.94 for 51 degrees of freedom, and the photon index is 2.25 ± 0.15. The ratio of the data to the power law plus Galactic absorption model is shown in Figure 5. This figure shows that there are no residuals that suggest a more complex model, and indeed, because the reduced χ^2 is less than one, a more complex model would overparameterize the data and would not be justified statistically. It is important to note that this photon index is consistent with the average hard X-ray photon index observed in *ASCA* spectra from NLS1s (2.19 ± 0.10; Leighly 1999b). Thus, PHL 1811 resembles an average NLS1 without a soft excess. The power-law X-ray spectrum is believed to be produced by Compton upscattering of soft photons in a hot plasma. This is the same process believed to operate in AGNs in general; the reason that the photon index is steeper in NLS1s than in broad-line quasars is that the hot plasma has been Compton cooled (e.g., Pounds et al. 1995).

Is the lack of complexity in the PHL 1811 spectrum due to the low flux and poor statistics, or does it really have a simple spectrum? We can obtain some answers to this question by extracting sufficiently short segments of *XMM-Newton* data from other NLS1s so that we obtain spectra with approximately 611 photons between 0.3 and 5 keV. We perform this exercise on two NLS1s: Ton S180 and 1H 0707−495.

Ton S180 has a spectrum with a mild soft excess. Vaughan et al. (2002) model it using a dual Comptonization model, and it was classified by Gallo (2006) as an NLS1 with a "simple" spectrum. The Ton S180 data are seen in the middle panel of Figure 5. This object is so bright that we need an exposure of just 51.52 s to obtain 572 photons between 0.34–5.61 keV (the observed-frame range corresponding to the rest-frame range of 0.36–5.96 keV for this $z = 0.062$ object). We fit the spectrum with a power law plus Galactic absorption and obtain a good fit, with a photon index of $3.04^{+0.17}_{-0.16}$ and $\chi_\nu^2 = 0.99$ for 33 degrees of freedom. The fact that the reduced χ^2 is less than one means that there is no statistical evidence for spectral complexity; in addition, we see no suggestive residuals in the data-to-model ratio. However, in contrast to PHL 1811, the photon index is significantly steeper than the average from NLS1s observed by *ASCA*, clearly because in this spectrum we are fitting the soft excess component predominantly. If this were the only X-ray spectrum that we had of this object, we would suspect that spectral complexity may be present and a hard tail might be seen in a longer observation, as it is (Vaughan et al. 2002).

1H 0707−495 has a complex spectrum that was modeled by Gallo et al. (2004b) using partial covering, and was classified by Gallo (2006) as an NLS1 with a "complex" spectrum. Note that this is the class that Gallo (2006) observes to be somewhat X-ray weak. The 1H 0707−495 data are seen in the bottom panel of Figure 5. In this case, a segment 289 s in length yielded a spectrum with 602 photons between 0.34 and 5.73 keV (the observed-frame range corresponding to the rest-frame range of 0.36–5.96 keV for this $z = 0.041$ object). We fit the spectrum with a power law plus Galactic absorption. In this case, the resulting photon index is even steeper than for Ton S180 ($\Gamma = 4.17^{+0.18}_{-0.17}$), the reduced χ^2 is significantly greater than 1 ($\chi_\nu^2 = 1.61$ for 34 degrees of freedom), and significant residuals are seen in the ratio. Clearly, despite the poor statistics in the spectrum, the need for a complex model is evident. It is also clear that although this object is X-ray weak, the X-ray spectrum is very dissimilar to that of PHL 1811.

This exercise shows that the X-ray spectrum of PHL 1811 is clearly different from those of two other NLS1s, Ton S180 and 1H 0707−495. These objects are representative of the complexity of spectra from NLS1s observed by *XMM-Newton*. The *XMM-Newton* spectrum from PHL 1811, a simple power law with a photon index consistent with the mean hard X-ray index from NLS1s observed by *ASCA*, suggests that the X-ray emission mechanism is simple Compton upscattering of soft photons in a hot plasma, as in other AGNs, and that the spectrum is unaltered by any extrinsic effects such as partial covering or reflection.

It may also be important that PHL 1811 is more UV-luminous than other NLS1s. The monochromatic luminosity at 2500 Å is

TABLE 4
Swift UVOT Results

Observation	Flux Density (10^{-14} erg s^{-1} cm^{-2} Å^{-1})[a]					
	UVW2	UVM2	UVW1	*U*	*B*	*V*
2005 Oct 22.....	3.75 ± 0.03	2.75 ± 0.02	2.45 ± 0.02	...	...	...
2006 May 12.....	3.66 ± 0.03	2.71 ± 0.03	2.47 ± 0.03	1.89 ± 0.04	0.99 ± 0.02	0.61 ± 0.02

[a] Observed fluxes; uncorrected for Galactic reddening.

30.9 (Paper II); thus, it is seen to be about 5 times more luminous than the most luminous object shown in Figure 2 of Gallo (2006). Also note that a very similar figure is shown in Leighly (2001) and Matsumoto et al. (2004).

2.5. *Swift Observations and Analysis*

PHL 1811 was observed by the *Swift* Gamma-Ray Burst Explorer Mission (Gehrels et al. 2004) on 2005 October 22 starting at 09:52 UT for a total of 2.5 ks. The observations were performed simultaneously with the X-Ray Telescope (XRT; Burrows et al. 2005) in the 0.3–10.0 keV energy range and the UV-Optical Telescope (UVOT; Roming et al. 2005) in the 1700–6500 Å wavelength range. It was observed again on 2006 May 12 for 1.6 ks. The details of the observations are given in Table 1.

The XRT data reduction was performed by the task `xrtpipeline`, version 0.9.9, which is included in the HEAsoft package, version 6.0.4. Source photons were selected in a circle with a radius of 23.4″ and the background photons in a source-free region close by with a radius of 95″. Those photons were extracted and read into separate event files with XSELECT, version 2.3. Twenty-two photons were detected during the first observation, and 10 were detected during the second observation for count rates of $(8.8 \pm 1.9) \times 10^{-3}$ s^{-1} and $(6.2 \pm 2.0) \times 10^{-3}$ s^{-1}, respectively.

In the 2005 October 22 observation, the UVOT photometry was performed with the UV filters UVW1, UVM2, and UVW2. During the 2006 May 12 observation, all six (optical and UV) filters were used. The details are given in Table 1. After the aspect correction the exposures in each filter were co-added into one image with `uvotimsum`, and the magnitudes and fluxes in each filter were determined with the task `uvotsource`. The results (observed fluxes, uncorrected for Galactic reddening) are listed in Table 4.

2.6. *MDM Optical Photometry*

Optical photometry data were taken on PHL 1811 at MDM Observatory using the 1.3 m McGraw-Hill telescope on the nights of 2004 October 14, 15, and 16 as part of a project to search for optical variability in the narrow-line quasar PHL 1092 (Gallo et al. 2004a). We used the thinned CCD "Templeton" and the telescope in the f/7.6 configuration, yielding a angular size of 0.50″ pixel^{-1}. The weather was good on October 14, with typical seeing of 1.7″, although the sky was not photometric. The seeing was worse on October 15 (average of 2.3″) and it was intermittently cloudy. On October 16, the weather had deteriorated further, and few usable frames were obtained.

We observed PHL 1811 using the *I*, *V*, *B*, and *U* filters, obtaining several exposures in each filter. The total number of frames analyzed were 9, 19, 12, and 11 for the *I*, *V*, *B*, and *U* filters, respectively. Within each night, the observations were all obtained within a time span of about 30 minutes, so we could test the interday optical variability principally between October 14 and October 15, as the sampling and data quality was much worse on October 16.

The images were reduced using standard IRAF procedures. Aperture photometry was performed on PHL 1811 and four field stars using an aperture twice the size of the image PSF FWHM. The aperture was chosen to ensure that essentially all of the photons from the object were measured, especially in cases where the image was slightly trailed due to clouds and loss of tracking. The ratio between PHL 1811 and the field stars was computed and errors were propagated. PHL 1811 is a bright object, so the mean signal-to-noise ratios in these ratios are high, ranging from 50 to 210.

We tested for variability in the ratio light curves using the "excess variance," a technique commonly used in X-ray astronomy. The excess variance is a measure of the observed variance in the light curve subtracting the variance due to measurement errors. In nearly all cases, this measure was negative. We conclude that no evidence for optical variability was found.

3. LONG TIMESCALE X-RAY AND UV VARIABILITY

PHL 1811 has now been observed in the X-ray bandpass seven times between 1990 and 2006: during the *ROSAT* All Sky Survey, by *BeppoSAX* in 2000 (Leighly et al. 2001), and in the two *Chandra* observations, the *XMM-Newton* observation, and the two *Swift* observations reported here. In Figure 6 we show the long-term light curve composed of the secure measurements, i.e., the last five observations. We do not plot the RASS upper limit or the *BeppoSAX* observation that, with the large detector PSF, was certainly contaminated by X-ray emission from neighboring objects. For the *Chandra* and *XMM-Newton* observations, the X-ray flux densities

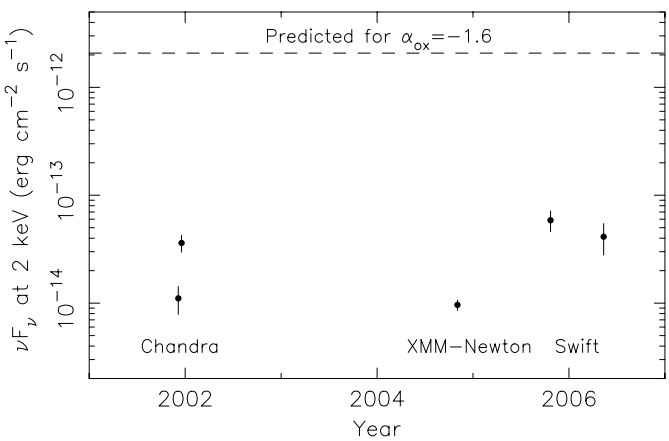

Fig. 6.—Long-term X-ray flux variability of PHL 1811 in terms of νF_ν at 2 keV in the rest frame. The uncertainties for the spectroscopic data (*Chandra* and *XMM-Newton*) are propagated 1 σ errors in the power-law normalization and index. For the detection data (*Swift*) the uncertainties are proportional to the count rate error. Note the logarithmic flux axis. Also shown is the predicted flux for $\alpha_{ox} = -1.6$ based on the UV flux from the *HST* observations.

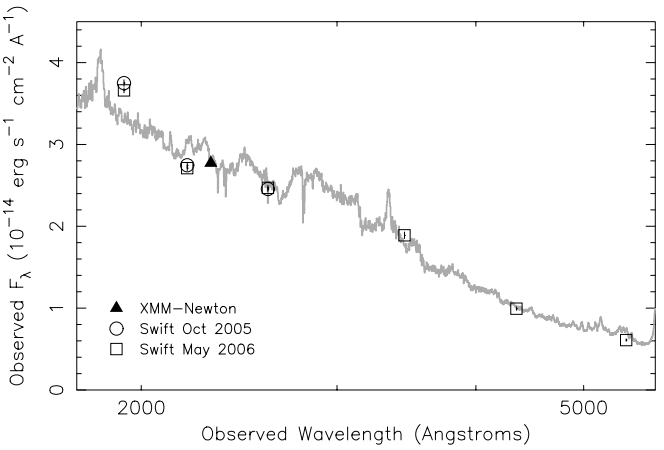

FIG. 7.—*XMM-Newton* OM and *Swift* UVOT photometry points overlaid on the observed merged optical and *HST* UV spectrum observed 2001 December 3 and discussed in Paper II. No strong evidence for UV variability is seen among the observations, which span 4.5 yr.

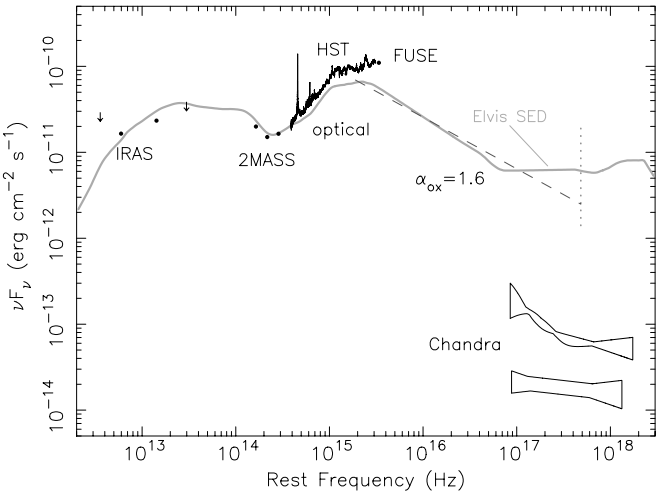

FIG. 8.—Spectral energy distribution of PHL 1811, plotted as a function of the rest-frame frequency. Contours from each of the two *Chandra* observations are shown, generated by successively setting each parameter to its $\Delta\chi^2 = 2.71$ value and computing the model, then determining the maximum and minimum of all of the models. The dashed line shows the expected 2 keV flux for an average quasar of this luminosity, based on the regression presented by Wilkes et al. (1994), while the dotted line shows the range observed by Wilkes et al. (1994). The average quasar SED from Elvis et al. (1994) scaled to the 1 μm inflection is also shown.

were estimated from the best-fitting power-law models, and the uncertainties were obtained by propagation of the errors on the normalizations and photon indices. For the *Swift* observations, the flux densities were estimated from the count rates using PIMMS,[7] assuming the *XMM-Newton* photon index ($\Gamma = 2.3$) and Galactic absorption, and the uncertainties in the flux densities were assumed proportional to the uncertainty in the count rate.

We find that PHL 1811 has varied significantly by a factor of $\sim$5 in this time period. The first *Chandra* observation and the *XMM-Newton* observation found it to be in a relatively low state, with νF_ν at 2 keV rest frame equal to $\sim 1.0 \times 10^{-14}$ erg s^{-1} cm^{-2}; the fluxes in these two observations are consistent with each other. The second *Chandra* observation and the two *Swift* observations show a significantly higher flux by a factor of 3.5–5.5, and the fluxes of these three are roughly consistent with one another, although the uncertainties are evaluated differently. Although there are only five points, these data suggest that the X-ray flux oscillates between two states that differ by a factor of 4–5. The NLS1 1H 0707−495 seems to behave the same way, oscillating between two flux states that differ by a factor of $\sim$10 (Leighly et al. 2002).

As will be discussed in § 4, quasars with PHL 1811's optical luminosity are statistically expected have values of α_{ox}[8] equal to −1.6. The dashed line in Figure 6 shows the predicted X-ray flux for $\alpha_{ox} = -1.6$ based on the UV flux of the *HST* spectrum. Although PHL 1811 varies significantly, it never approaches the nominal X-ray flux for an object of its UV luminosity.

We have four epochs of UV observations: the *HST* STIS spectroscopic observation made 2001 December 3 (discussed in detail in Paper II), the *XMM-Newton* OM observation made 2004 November 1, and the two *Swift* UVOT observations made 2005 October 22 and 2006 May 12. We search for possible UV variability by comparing the latter three photometry measurements with the *HST* spectrum.

The effective wavelength of the *XMM-Newton* OM UVM2 filter is 2310 Å. We plot the observed fluxes on the observed-frame merged *HST* and optical spectrum from Paper II in Figure 7. We find that the photometry flux is completely consistent with the observed spectrum.

The effective wavelengths of the *Swift* UVOT photometry points are listed in Table 1, and the inferred fluxes are plotted in Figure 7. Note that the filter transmission functions in the *Swift* UVOT are different from those in the *XMM-Newton* OM, even though the filter names are the same; hence, the effective wavelengths are somewhat different. Like the *XMM-Newton* OM photometry, the correspondence between the UVOT photometry and the *HST* spectrum is very good, with the exception of the photometry using the UVW2 filter. That filter is especially difficult to calibrate as the complete filter transmission curve is not known[9] and because of the paucity of suitable calibration targets. Therefore, we do not consider the disagreement with the *HST* spectrum indicative of a spectral change. We conclude that we observe no evidence for any UV variability between the four UV observations that span a time period of 4.5 yr.

To summarize, PHL 1811 has now been observed seven times in the X-rays over a period spanning 16 yr. During this time, the X-ray flux has been observed to vary by a factor of $\sim$5, but it remains well below that of a typical quasar of its UV luminosity. In contrast, the four UV observations made over a period of 4.5 yr do not show any convincing evidence of UV variability.

4. THE SPECTRAL ENERGY DISTRIBUTION

We presented the first spectral energy distribution of PHL 1811 in Leighly et al. (2001) based on an optical spectrum, a *ROSAT* upper limit, a *BeppoSAX* observation, and multiwavelength photometry. In Figure 8, we present an updated spectral energy distribution. For the optical and UV, we used the merged spectrum described in Paper II. The *Chandra* results are represented by regions on the SED plot that were constructed using the third joint model fit (Table 2). The contours were constructed by successively setting each variable parameter to its $\Delta\chi^2 = 2.71$ value and computing the model, then determining the maximum and minimum of all the models.

[7] Available at http://cxc.harvard.edu/toolkit/pimms.jsp.

[8] The parameter α_{ox} is defined as the point-to-point slope between 2500 Å and 2 keV; i.e., $\alpha_{ox} = \log(F_{2500}/F_{2\,keV})/2.61$.

[9] See http://swift.gsfc.nasa.gov/docs/heasarc/caldb/swift/docs/uvot/uvot_caldb_filtertransmission_02.pdf.

From the best-fit *Chandra* model and the merged *HST* and optical spectrum, we compute α_{ox} to be -2.40 for the first observation, which was nearest in time to the *HST* observation, and -2.19 for the second observation. As seen in Figures 6 and 7, the *Chandra* and *HST* fluxes are comparable with the *XMM-Newton* and *Swift* fluxes, so we confine our discussion to the *Chandra* and *HST* data here without loss of generality.

Wilkes et al. (1994) computed a regression between optical luminosity and α_{ox} for a heterogeneous sample of quasars. Using their cosmology ($H_0 = 50$ km s^{-1} Mpc^{-1}, $q_0 = 0$), we obtain a luminosity distance for PHL 1811 of 1261 Mpc and a corresponding luminosity density at 2500 Å of 1.44×10^{31} erg s^{-1} Hz^{-1}. Then using their regression, we predict α_{ox} to be -1.6. We plot the predicted X-ray flux assuming this value of α_{ox} on Figure 8, as well as a vertical bar that indicates the range of X-ray luminosities observed by Wilkes et al. (1994).

More recently, Strateva et al. (2005) and Steffen et al. (2006) updated the α_{ox} regression using a large sample of optically selected active galaxies that span a large range in redshift and luminosity yet have highly complete X-ray data. For their cosmology ($H_0 = 70$ km s^{-1} Mpc^{-1}, $\Omega_M = 0.3$, and $\Omega_\Lambda = 0.7$) we obtain a luminosity distance of 936 Mpc and a corresponding luminosity density at 2500 Å of 7.92×10^{30} erg s^{-1} Hz^{-1}. Their regression yields a predicted α_{ox} of -1.60 as well. From their Figure 4, we find that the envelope of α_{ox} observed for quasars of this luminosity spans approximately -1.75 to -1.4. Our observed X-ray luminosity densities are factors of 130–450 below the high value and 13–45 below the low value. Thus, PHL 1811 is observed to be significantly X-ray weak compared with other quasars.

Brandt et al. (2000) compile the distribution of α_{ox}[10] from the PG quasar sample studied by Boroson & Green (1992). They find a suggestion of a bimodal distribution with 10 of the 87 objects classified as X-ray weak with $\alpha_{ox} \leq -2$. Then they find a connection between α_{ox} and the presence of significant C IV absorption lines, such that most of the soft X-ray weak objects have absorption-line equivalent widths greater than 5 Å. They infer these results to imply that X-ray absorption is the primary origin of soft X-ray weakness in AGNs.

Clearly PHL 1811 does not follow the trend observed by Brandt et al. (2000). It is soft X-ray weak, but, as discussed in Paper II, there is no evidence for any significant intrinsic C IV absorption lines. In the Brandt et al. (2000) sample, objects with similar α_{ox} as observed from PHL 1811 have C IV absorption line equivalent widths of 5–20 Å.

Furthermore, the X-ray spectrum shows no evidence for intrinsic absorption. If low–column-density absorption were present, we would expect to observe a flat spectrum; in contrast, for a single power-law model, we measure photon indices of 2–2.6, consistent with unabsorbed quasars, and an upper limit on intrinsic absorption of 8.7×10^{20} cm^{-2}.

Another possibility is that a high–column-density or Compton-thick absorber is present in our line of sight, so that we see no direct continuum emission. Our spectra do not probe high enough energies to see whether there is a highly absorbed component, as has been found in broad absorption line quasars (BALQSOs; e.g., Gallagher et al. 2002; Green et al. 2001). If the continuum emission were completely absorbed, then the X-ray spectrum that we see might have been scattered into our line of sight (i.e., similar to a Seyfert 2 galaxy or BALQSO). Electron scattering is energy independent, so in this scenario we would expect to see the intrinsic power law with attenuated flux. In Seyfert 2s, the electron scattering occurs over an extended area, and thus while the intrinsic X-ray emission may vary, the scattered emission does not, because variability is washed out as it scatters over the extended region. The fact that we see significant variability between the two *Chandra* observations, separated by 12 days, argues that we are not seeing scattered light. This conclusion depends on the compactness of the electron-scattering mirror; if unusually compact, observation of variability would be possible. Regardless, the observation of significant variability between two observations separated by 12 days from this luminous quasar suggests that we are seeing the intrinsic emission from the AGN.

Narrow-line Seyfert 1 galaxies are known for their high-amplitude X-ray variability (e.g., Leighly 1999a). As discussed in Leighly et al. (2001) it was possible, at that time, when we had only the RASS upper limit and the *BeppoSAX* data, that we had coincidentally only observed PHL 1811 while it was in a transient low state. In this paper, we report five more X-ray observations, all of which find it to be a significantly weak X-ray source. Thus, the probability that we coincidentally observe it in a low state is decreasing. PHL 1811 appears to be intrinsically X-ray weak.

5. DISCUSSION

5.1. *PHL 1811 is Intrinsically X-Ray Weak*

In Leighly et al. (2001) we reported the first X-ray detection of PHL 1811 by *BeppoSAX*. That observation showed that PHL 1811 appeared to be X-ray weak, but the 65 net photon spectrum was not sufficient to determine the origin of the X-ray weakness. We presented three alternatives for the X-ray weakness: (1) PHL 1811 is a BALQSO, and the X-ray emission is absorbed; (2) since PHL 1811 is an NLS1, it is highly X-ray variable, and we happened to catch it in a low state; or (3) PHL 1811 is intrinsically X-ray weak. The *HST* observation discussed in Paper II and the *Chandra* observations reported here show that it is not a BALQSO, as there is no evidence for UV absorption lines. Furthermore, there is no evidence for absorption in the X-ray spectrum, and the significant variability between the two *Chandra* observations suggests that the X-ray emission is not scattered. So the first hypothesis is firmly ruled out.

We can never conclusively rule out the second hypothesis, that PHL 1811 is highly X-ray variable and we always just happen to catch it in a low state. However, it has now been observed seven times between ~1990 (during the *ROSAT* All Sky Survey) and 2006 May (in a *Swift* observation), and it has never been observed to be bright. In fact, since it has already varied by a factor of ~5 among the observations reported here, it may have already been as bright as it can get. It seems increasingly unlikely that it will ever be as X-ray bright as other quasars.

Thus, we conclude PHL 1811 is intrinsically X-ray faint. Most quasars are bright X-ray sources, so what property of the PHL 1811 central engine causes it to be X-ray faint? As we pointed out in Leighly et al. (2001; also Grupe et al. 2001), there is no obvious reason why intrinsically X-ray weak quasars should not exist. Briefly, a quasar arguably cannot exist without accretion as a source of fuel. In an object such as PHL 1811, that accretion probably occurs through an optically thick, geometrically thin accretion disk that emits the observed strong optical and UV continuum (Fig. 8). Such a disk would never be hot enough to emit X-rays, which are probably emitted by the corona, a separate component. We postulated that there may be situations in which the corona may not exist or may be weak.

[10] Brandt et al. (2000) use an alternative definition of α_{ox} using the flux density at 3000 Å rather than 2500 Å. They estimate that $\alpha_{ox}(2500) = 1.03\alpha_{ox}(3000) - 0.03\alpha_u$, where α_u is the slope of the spectrum between 2500 and 3000 Å.

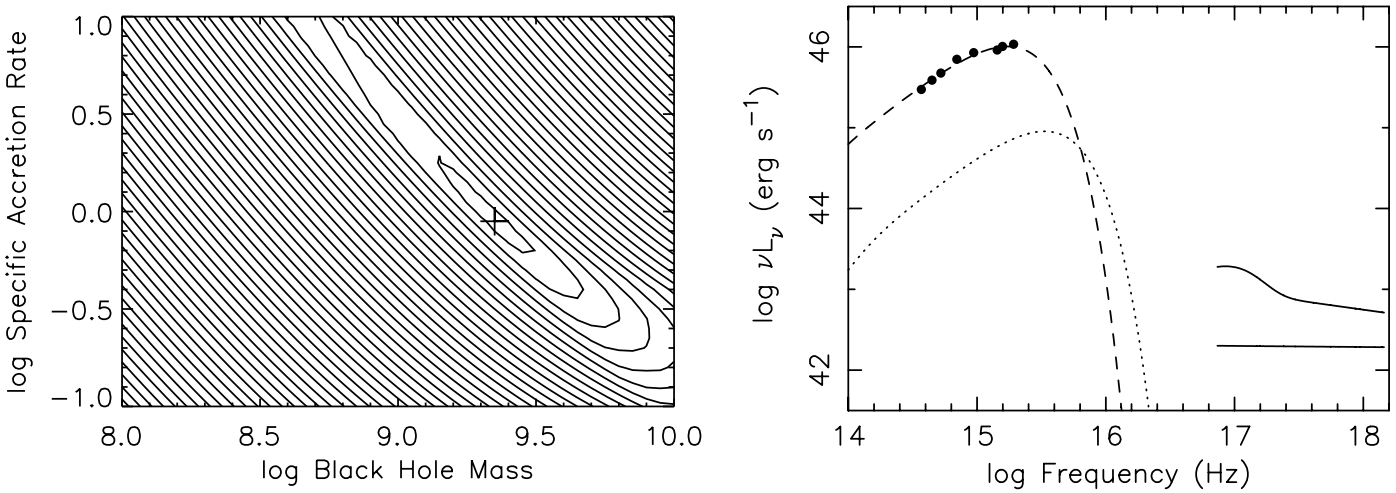

FIG. 9.—*Left*: Contours of equal deviation of UV flux points from sum-of-blackbodies accretion disk models, as a function of input black hole mass (in units of solar masses), and the specific accretion rate, $\dot{m}$. See text for further information. The contour interval is 0.05 in units of log νL_ν. The minimum is located at $M_{\rm BH} = 2.2 \times 10^9\ M_\odot$ and $\dot{m} = 0.9$. *Right*: UV continuum flux points (*filled circles*) and X-ray spectra (*solid lines*). The best-fitting model is shown by the dashed line. For comparison, the spectrum for a $M_{\rm BH} = 1.8 \times 10^8\ M_\odot$ black hole with $\dot{m} = 1.0$ is shown by the dotted line.

Why might the corona be weak? As discussed in Leighly et al. (2001) PHL 1811 is a very luminous NLS1. As discussed by Laor (2000) narrow Balmer lines in luminous AGNs may imply high accretion rates if the width of the lines is dominated by virial motions. One possible central engine geometry considers the X-rays to be emitted by a central, hot, optically thin, geometrically thick disk, and the optical and UV emitted by an optically thick, geometrically thin disk with a large inner radius (e.g., Zdziarski & Gierlinski 2004). At high accretion rates, it might be expected that the inner radius of the optically thick, geometrically thin disk would shrink down toward the innermost stable orbit, with the volume of the central hot X-ray emitting region shrinking with it, and the intensity of the X-ray emission correspondingly decreasing. This is thought to happen in Galactic X-ray transient objects (e.g., Kubota & Done 2004).

Alternatively, the corona may lie on top of the optically thick, geometrically thin accretion disk and be fed by reconnecting magnetic flux tubes buoyantly emerging from the disk. Decreasing the amount of energy released by reconnection in PHL 1811 would result in weak X-ray emission. Why would that happen? One model, proposed by Bechtold et al. (2003), explains the dependence of $\alpha_{\rm ox}$ on luminosity in the context of a disk/corona model in which the two phases are thermally coupled and in which the amount of energy dissipated into the corona depends on the gas pressure in the disk. In this model, $\alpha_{\rm ox}$ is steeper for larger black holes, larger accretion rates with respect to Eddington, and larger viscosity parameters.

It is also possible that since the optical-UV spectrum is very soft, softer than most quasars, the corona is flooded by soft photons, catastrophically Compton cooling it, and so reducing the X-ray emission. This idea is discussed by Proga (2005), who suggests that a luminous accretion disk can simultaneously drive an outflow and quench the corona. This idea is supported by the fact that we see blueshifted high-ionization lines in PHL 1811 (discussed in Paper II) and by the observed inverse correlation between $\alpha_{\rm ox}$ and the blueshift of C IV lines among NLS1s (Leighly & Moore 2004).

Another way that a high accretion rate may lead to reduced X-ray emission is through so-called photon trapping. If the accreting gas is simply free-falling into the black hole, the photons may be accreted before they can diffuse out through the accreting gas when the accretion rate is high; they are trapped and advected into the black hole (Begelman 1978). Because the X-rays are most likely to be emitted very close to the black hole, more of them could be trapped than optical/UV photons, resulting in a steep $\alpha_{\rm ox}$.

5.2. *The Black Hole and Accretion Disk in PHL 1811*

It is generally thought that the source of the optical-UV bump in AGN broadband spectra is thermal emission from the accretion disk that powers the active nucleus. Despite this conviction, results from observations of the optical-UV properties in AGNs do not conform to our expectations of accretion disks; specifically, the continuum does not have the expected slope, the disk emission does not appear to be polarized, and there is no prominent Lyman edge feature (Koratkar & Blaes 1999). PHL 1811 has a prominent big blue bump (Fig. 8); in this section we explore the accretion disk explanation for this feature.

The simplest model of an accretion disk is constructed by assuming that half of accretion energy heats the disk, and the disk radiates locally like a blackbody (e.g., Frank et al. 1992). This model has the advantage that it is easy to compute, but the disadvantage that is not thought to be physically realistic. As shown below, however, we can obtain some useful results by quantitatively comparing this model with our data.

We compute the spectra emitted by the accretion disk between $R = 3.1R_{\rm S}$ and $1000R_{\rm S}$ in the frequency range log (ν) = 14–19 (Hz), for a range of black hole masses between 10^7 and $10^{11}\ M_\odot$ and a range of specific accretion rates, $\dot{m} = \dot{M}/\dot{M}_{\rm Edd}$, between 0.1 and 10, noting that this simple geometrically thin, optically thick model should break down at the higher specific accretion rates. We assume that the disk is observed face-on ($\cos i = 0$). To compare the accretion disk spectra with our data, we identify regions of the merged optical and UV spectrum that appear not to be dominated by emission lines and obtain the average flux in these bands.[11] We then compute the sum of the mean deviation of $\log(\nu L_\nu)$ at the mean frequencies for each band from each model. The contours of the mean deviation are shown in the left panel of Figure 9. We find that only a relatively

[11] The bands we use are 1089–1102, 1317–1352, 1460–1482, 2229–2244, 3011–3038, 4014–4058, 4698–4768, and 5700–5750.

small range of $M_{\rm BH}$ and $\dot{m}$ match the data. The best-fitting values are $M_{\rm BH} = 2.2 \times 10^9\ M_\odot$ and $\dot{m} = 0.9$. The best-fitting continuum spectrum is seen in the right panel of Figure 9.

What is the mass of the black hole in PHL 1811? We can estimate the mass using any number of the relationships between mass, Hβ velocity width, and νL_ν at 5100 Å currently available. We use that given by Vestergaard & Peterson (2006). We measure λL_λ(5100 Å) to be 3.6×10^{45} erg s^{-1} using a distance of 936.4 Mpc. We note that the flux from the merged spectrum appears to be consistent with the broadband photometry. The mean flux density over a 980 Å band centered at observed 4400 Å is 1.0×10^{-14} erg s^{-1} cm^{-2} Å^{-1}. The photometry value, $B = 14.4$, corresponds to 1.15×10^{-14} erg s^{-1} cm^{-2} Å^{-1}, and so is consistent within 15%. Given that the observations were not contemporaneous, this is quite good agreement. As will be discussed in Paper II, we measure the width of Hβ to be 1943 km s^{-1}. Using equation (5) of Vestergaard & Peterson (2006), we find the black hole mass to be $1.8 \times 10^8\ M_\odot$, a factor of 12 smaller than the estimate based on the accretion disk model above. Thus, the disk must be radiating at a rate significantly higher than the Eddington value to attain the luminosity in the optical-UV band pass that we observe. To illustrate this, we plot the spectrum for $M_{\rm BH} = 1.8 \times 10^8\ M_\odot$ and $\dot{m} = 1.0$ on Figure 9.

It is worth pausing to note that there are several reasons why this may not be an accurate estimate of the black hole mass in very peculiar objects such as PHL 1811. As is discussed in the introduction of Vestergaard & Peterson (2006) and references therein, there are a number of assumptions and suppositions that go into the construction of reverberation-based black hole masses. The primary assumption is that the line widths are virial. The evidence that this is true comes from a very few Seyfert 1.5 galaxies with excellent multiwavelength monitoring data (Peterson & Wandel 2000). Narrow-line Seyfert 1s such as PHL 1811 are different from these objects in that their Hβ lines do not seem to vary, although variability has been observed in low-luminosity NLS1s such as NGC 4051. The other evidence that the line widths are virial comes from the fact that in lower luminosity reverberation-mapped AGNs, the black hole mass estimated from the line widths and continuum luminosity is consistent with that estimated from the host galaxy stellar velocity dispersion and the $M_{\rm BH}$-σ relationship. PHL 1811 is much different from these objects as it has a much higher luminosity. The uncertainty in the black hole mass in the reverberation-mapped objects is given to be a factor of $\sim$2.9 based on the scatter around the $M_{\rm BH}$-σ relationship (Onken et al. 2004). However, the deviation from the reverberation-mapping black hole mass in PHL 1811 may be larger for several reasons. First, it is possible that the broad-line regions in narrow-line Seyfert 1s have a flattened configuration; this has been previously suggested by McLure & Dunlop (2002). A flatter distribution in NLS1s would decrease the observed velocity width and could also naturally yield the observed lower equivalent widths as a consequence of a smaller covering fraction. This might imply a larger black hole mass in PHL 1811 than estimated by the regressions based on reverberation-mapped AGNs. On the other hand, PHL 1811 has a soft spectral energy distribution. This means that it produces a weaker ionizing continuum compared with other quasars with similar optical luminosity. Inverting the argument originally made by Wandel & Boller (1998; applied to NLS1s that were inferred to have a stronger ionizing continuum because of their prominent soft excess), this implies that the Hβ lines should be produced closer to the continuum source than in other NLS1s, which would require the black hole mass to be smaller. The point is that extrapolating the relationships obtained from the reverberation-mapped AGNs may be particularly dangerous for extreme objects such as PHL 1811.

Regardless, assuming the black hole mass estimated above, we infer that the disk must be radiating at a rate very much higher than the Eddington value to attain the observed optical-UV luminosity. We note we are not the first to infer super-Eddington radiation in NLS1s; this was also found by Collin & Kawaguchi (2004) using a different approach. They estimated the black hole masses from the Hβ line widths and then compared the observed bolometric luminosity to the predicted one, whereas we instead compare the luminosity and shape of the accretion disk to the observed continuum.

What is the bolometric luminosity of PHL 1811? We integrate over the inferred broadband continuum to determine this. For wavelengths shorter than 1 μm, we use the spectral energy distribution inferred from the observed optical, UV, and X-ray data. It is composed of piecewise power laws, suitable for use in Cloudy, and can be seen in Figure 12 of Paper II. Longward of 1 μm, we use the Elvis et al. (1994) average continuum spectrum, since it is seen to match the 2MASS and *IRAS* photometry rather well (Fig. 8). The result is 3.7×10^{46} erg s^{-1}. It is 10.2 times λL_λ(5100), and so $L_{\rm bol}/\lambda L_\lambda$(5100) is very close to 9, the bolometric correction factor often used for AGNs (and assumed in the mass-luminosity relationship in Peterson et al. 2004).

The Eddington luminosity for a $1.8 \times 10^8\ M_\odot$ black hole is 2.25×10^{46} erg s^{-1}. This implies that PHL 1811, overall, is radiating at about 1.6 times the Eddington luminosity. But as the accretion disk fits show, the optical-UV region is radiating at a very super-Eddington rate.

The sum-of-blackbodies spectrum is not a physically realistic model for an AGN accretion disk, although since it is the sum of blackbodies, it will be the overall *brightest* disk for a homogeneous, isotropically emitting disk. It does not take into account vertical disk structure, Comptonization, or other effects that are expected to influence the disk spectrum. What do we expect to see from a realistic accretion disk spectrum in comparison with the sum-of-blackbodies model?

Shimura & Takahara (1993, 1995) considered the effect of vertical structure and radiative transfer in the accretion disk and applied their results to AGN and black hole candidates. They found that the emerging spectrum is significantly harder than the sum-of-blackbodies disk, due to electron scattering and the vertical temperature gradient. This means that for a given accretion rate and black hole mass, their computed disk spectrum has proportionally more soft X-rays than the sum-of-blackbodies disk, but at the expense of the UV. In order for the flux of such a disk spectrum to match the UV flux from PHL 1811, an even larger black hole would be necessary. In fact, this should be generically true for any disk model that radiates at less than the Eddington rate (e.g., Kawaguchi et al. 2001).

More recently, models for disks with super-Eddington emission have been proposed by several authors (e.g., Begelman 2002). In the Begelman (2002) model, the disk is inhomogeneous, and radiation leaks out through optically thin channels. We infer that PHL 1811 is radiating at a super-Eddington rate in the optical and UV. Perhaps this means that the spectrum of a super-Eddington disk should be similar to that of a typical quasar longward of $\sim$1550 Å, based on Figure 8 of Paper II. One might expect the super-Eddington emission to be stronger closer to the black hole, where the shorter wavelength emission originates. Perhaps this is the origin of the unusual rising continuum shortward of $\sim$1400 Å shown in Figure 8 of Paper II.

5.3. *The Host Galaxy of PHL 1811*

Magorrian et al. (1998) discovered that black hole masses are correlated with the luminosity of the host bulge or elliptical galaxy. Later it was found that a tighter correlation between the velocity dispersion of the bulge of a galaxy and the mass of the nuclear black hole exists (Ferrarese & Merritt 2000; Gebhardt et al. 2000). The host galaxies of luminous active galaxies, i.e., quasars, are almost exclusively ellipticals, and their basic properties are the same as elliptical galaxies without quasars (e.g., Dunlop et al. 2003). Furthermore, they obey the relationship between black hole mass and spheroid mass observed in nearby galaxies (e.g., Dunlop 2004). PHL 1811 has a rather large black hole ($\sim 1.8 \times 10^8\ M_\odot$; § 5.2) and therefore should have a large elliptical galaxy as a host. An object that should in principle be quite similar is the quasar 3C 273. Its redshift is 0.158 and its black hole mass is inferred to be $8.8 \times 10^8\ M_\odot$ (Peterson et al. 2004). Martel et al. (2003) present the ACS coronagraph data from this object. They find a large elliptical galaxy with an inner region about 17 kpc in diameter (6.5″) and extended diffuse emission out to 6″–12″ from the active nucleus. A de Vaucouleurs fit to the *V* and *I* profiles yields effective radii of ∼2.2″ and ∼2.6″.

Jenkins et al. (2005) show an *HST* ACS WFC image of PHL 1811. Observations of the host galaxies of nearby quasars are best done using the coronagraph; however, there was not sufficient time in that program to make the coronagraph image with an accompanying PSF calibration exposure. They instead made a 520 s observation directly using the F625W (Sloan r^*) filter and corrected for the QSO PSF using a nearby star with colors similar to those of PHL 1811. The resulting image was surprising; it does not show a large elliptical host like 3C 273; rather there are structures that look like spiral arms on either side of the QSO. These features are not an artifact of the PSF subtraction as they can even be seen in the image before subtraction, and for other reasons discussed by Jenkins et al. (2005). Thus, PHL 1811 appears to have a spiral host, and appears to lack a large bulge that might be expected given its luminosity.

The 3C 273 observations were 9–10 times longer than the PHL 1811 observations; perhaps the PHL 1811 image is not sufficiently well exposed to observe the bulge? We can estimate the expected properties of a typical host galaxy by using our black hole mass estimate to estimate the mass of the spheroid, then determining the expected observational properties of an elliptical galaxy having a spheroid of that mass.

In § 5.2 we showed that the luminosity of the optical-UV spectrum is consistent with a black hole of $2.2 \times 10^9\ M_\odot$. However, using the black hole mass based on AGN reverberation-mapping results given by Vestergaard & Peterson (2006), we obtain a much smaller black hole mass of $1.8 \times 10^8\ M_\odot$. Using the relationship between the black hole mass and the mass of the spheroid ($M_{\rm BH} = 0.0012 M_{\rm sph}$; Dunlop 2004) yields $M_{\rm sph} = 1.5 \times 10^{11}\ M_\odot$ for the estimated $M_{\rm BH} = 1.8 \times 10^8\ M_\odot$.

It has been found that the host galaxies of quasars are indistinguishable from elliptical galaxies. Therefore, we can use the properties of elliptical galaxies to estimate the size and brightness of the putative host. The mass of the spheroid is related to the effective radius by $r_e = 2.6 (M_{\rm sph}/10^{11})^{3/5}$ kpc for $H_0 = 70$ km s^{-1} Mpc^{-1} (Loewenstein & White 1999). Thus, for PHL 1811, we expect an effective radius of 3.3 kpc. At the distance of PHL 1811, 1″ corresponds to 3.2 kpc, so $r_e = 3.3$ kpc corresponds to 1″. The image presented by Jenkins et al. (2005) is not reliable within about 1.5″ due to the correction for the QSO PSF, but should be fine at $\sim 2 r_e$.

It is well known that the surface brightness of elliptical galaxies is correlated with the effective radius (e.g., Djorgovski & Davis 1987). There is, however, considerable scatter, although McLure & Dunlop (2002) argue that the rms scatter for AGN hosts is only 0.18 dex. We use the results from a recent analysis of elliptical galaxies in the Sloan Digital Sky Survey (Bernardi et al. 2003). For the effective radius of 3.3 kpc, their Figure 10 shows that the mean surface brightness is ∼20 mag arcsec^{-2}, and almost all objects lie within 19–21 mag arcsec^{-2} in the r^* filter. We need to account for cosmological dimming, which will lower the observed surface brightness by a factor of $(1+z)^4 = 2.02$. Then the mean surface brightness is 20.75 mag arcsec^{-2}, with a conservative range of 21.75–19.75 mag arcsec^{-2}.

Since the image is not reliable at $1 r_e$ due to PSF distortion, we need to estimate the surface brightness at $2 r_e$. Assuming a de Vaucouleurs profile, we can use this average to find the expected surface brightness at $2 r_e$ (e.g., Binney & Merrifield 1998). We then find the mean surface brightness to be 22.25 mag arcsec^{-2}, with a range of 23.25–21.25 mag arcsec^{-2}.

Next, we use the exposure time calculator for the *HST* ACS to determine the expected signal-to-noise ratio of diffuse emission obtainable in a 520 s exposure using the F625W filter. We use the built-in spectrum of an elliptical galaxy and include the effect of Galactic extinction by $E(B-V) = 0.046$. We find that the mean surface brightness of 22.25 mag arcsec^{-2} yields a signal-to-noise ratio in a 2×2 pixel box of 5.4, with a range of 2.3–11.7 for the surface brightness range. Thus, if PHL 1811 had a normal elliptical galaxy host, it may have been detected at $2 r_e = 2''$ in the Jenkins et al. (2005) image, assuming it is on the brighter side of the range of elliptical galaxies.

Finally, it has been found that NLS1s frequently have a much larger host galaxy bulge than expected based on their black hole mass estimated from their emission-line widths (e.g., Grupe & Mathur 2004; Mathur & Grupe 2005). In addition, Ryan et al. (2007) find from near-IR imaging of NLS1s that the bulge is about an order of magnitude larger than would be inferred using the $M_{\rm BH}$-σ relationship and the black hole masses estimated from reverberation mapping. If PHL 1811 had followed this trend, the host galaxy bulge should have been very easy to see.

6. SUMMARY

In this paper, we report the results and analysis of two *Chandra* observations that were coordinated with an *HST* observation, an *XMM-Newton* observation, two *Swift* ToO's, and MDM optical photometry of the unusually luminous, nearby narrow-line quasar PHL 1811. Here we summarize the primary results of the paper.

1. The two 10 ks *Chandra* observations, made 12 days apart, reveal a weak X-ray source at the position of PHL 1811. A factor of 4 variability was observed between the two observations. The X-ray spectrum is steep, with photon index $\Gamma \sim 2$–2.6, typical of the power-law indices observed in *ASCA* spectra from NLS1s. There is marginal evidence of a soft excess in the brighter spectrum, and marginal evidence for spectral variability in which the soft excess became more prominent when the object was brighter. No evidence for absorption was found.

2. The ∼30 ks *XMM-Newton* observation revealed no evidence for X-ray variability, and a flux consistent with the fainter of the two *Chandra* spectra. The X-ray spectrum is steep with $\Gamma = 2.3 \pm 0.1$, again typical of the power-law indices observed from NLS1s by *ASCA*. There is no evidence for absorption, with an upper limit on intrinsic absorption of 8.7×10^{20} cm^{-2}. The Optical Monitor data revealed no evidence for short timescale UV

variability. Two *Swift* observations found the flux to be consistent with the brighter of the two *Chandra* spectra. Overall, a factor of $\sim$5 variation in X-ray flux was observed among the five X-ray observations presented in this paper. The UV photometry, obtained by *XMM-Newton* and *Swift*, is consistent with the *HST* spectrum discussed in Paper II; thus, no evidence for UV variability has been found. In addition, MDM photometry observations revealed no evidence for optical variability over three nights.

3. We compare the *XMM-Newton* PN spectrum of PHL 1811 with those from two representative NLS1s: Ton S180, which has been previously modeled using a dual Comptonization model, and 1H 0707−495, which has been previously modeled using partial covering or a reflection model. Since the comparison NLS1s are much brighter than PHL 1811, we extracted spectra from sufficiently short segments that the number of photons in the PN spectra are approximately the same as in the PHL 1811 spectrum. Fitted with a power-law model, the comparison spectra are significantly steeper than that of PHL 1811, and complexity is detected in the spectrum from 1H 0707−495. PHL 1811's X-ray spectrum seems to be different from those of other NLS1s. Since the slope is consistent with the power law observed in *ASCA* spectra of NLS1s, the simplest explanation for the X-ray spectrum in PHL 1811 is that it is powered by Compton upscattering of soft photons by energetic electrons, the typical power-law X-ray emission mechanism in quasars.

4. The *BeppoSAX* observation found PHL 1811 to be significantly X-ray weak (Leighly et al. 2001). At that time, we presented three possible explanations for its X-ray weakness: (1) PHL 1811 is a BALQSO, (2) PHL 1811 is temporarily in a low-flux state, or (3) PHL 1811 is intrinsically X-ray weak. The spectral energy distribution, constructed using the *Chandra* spectra and the *HST* spectrum taken two days before the first *Chandra* observation, confirms that PHL 1811 is X-ray weak, with α_{ox} between -2.2 and -2.4. The *XMM-Newton* and *Swift* observations are consistent with these values. The α_{ox} for a typical quasar of similar UV luminosity is -1.6, and compared with a sample of optically selected quasars of similar UV luminosity, the X-ray flux of PHL 1811 is a factor of 13–450 times weaker. The lack of absorption in the X-ray spectra and the lack of absorption lines in the UV spectrum (Paper II) conclusively rule out the possibility that PHL 1811 is a BALQSO, with a weak, absorbed X-ray spectrum characteristic of that class of object. PHL 1811 has now been observed seven times in X-rays between 1990 (during the *ROSAT* All Sky Survey) and the most recent *Swift* observation on 2006 May 14. While it varies by about a factor of 5 among the latter five observations, ruling out a scattering origin for the X-ray emission from an extended electron-scattering mirror, it is always significantly weaker than other quasars of similar optical luminosity. While we can never rule out the possibility that PHL 1811 is coincidentally always observed when it is in a transient low state, the plausibility of this hypothesis is decreasing. We conclude that PHL 1811 is *intrinsically* X-ray weak.

5. We discuss the possible origins of the X-ray weakness. It may be a consequence of the high accretion rate inferred from the narrow lines and high luminosity. The corona may be smaller, and with a larger fraction of the accretion power going into the optically thick, geometrically thin accretion disk emitting the optical and UV continuum. Alternatively, the corona may be quenched by the strong optical and UV emission, and may be unable to Compton upscatter those photons to X-ray energies. Another possibility is that high accretion rate traps the X-ray photons and advects them into the black hole.

6. We compare the spectral energy distribution with a simple sum-of-blackbodies accretion disk model. We find that the UV spectrum is consistent with a black hole mass of $2.2 \times 10^9\ M_\odot$ and a specific accretion rate of $\dot{m} = 0.9$. Using the Hβ FWHM, the luminosity at 5100 Å, and an equation derived from results of reverberation-mapped AGNs given by Vestergaard & Peterson (2006), we obtain a black hole mass estimate of $1.8 \times 10^8\ M_\odot$, a factor of 12 below the value obtained from the accretion disk spectrum. We caution that we do not have a direct measurement of the black hole mass for this object. We point out that while the sum-of-blackbodies disk is not physically realistic, it is the brightest homogeneous, isotropically emitting disk, and most other, more realistic disks will require an even higher radiation rate relative to Eddington. The exception may be inhomogeneous disks recently proposed by, e.g., Begelman (2002) in which radiation leaks out through optically thin channels. Based on the observed broadband continuum spectrum, and extrapolating to the IR using the Elvis et al. (1994) SED, we estimate the bolometric luminosity to be 3.7×10^{46} erg s^{-1}. Thus, overall, PHL 1811 is radiating at 1.6 times the Eddington rate, with the optical and UV well above Eddington. We also discuss the *HST* ACS image presented by Jenkins et al. (2005) that reveals a spiral galaxy at the position of PHL 1811. Most quasars have elliptical hosts; we demonstrate that if PHL 1811 had the large elliptical host typical of average quasars with $1.8 \times 10^8\ M_\odot$ black holes, it might have been seen (i.e., the estimated signal-to-noise ratio is $\sim$5) in that image. A spiral host galaxy appears to be yet another unusual feature of PHL 1811.

K. M. L. acknowledges helpful conversations with Andrzej Zdziarski regarding accretion disks and Mike Loewenstein regarding elliptical galaxies. We thank the anonymous referee for helpful comments. Support for this work was provided by the National Aeronautics and Space Administration through *Chandra* Award GO2-3119X issued by the *Chandra* X-Ray Observatory Center, which is operated by the Smithsonian Astrophysical Observatory for and on behalf of the National Aeronautics Space Administration under contract NAS8-39073. K. M. L. and J. C. gratefully acknowledge support through grant NNG05GB38G (*XMM-Newton* Cycle 3 Guest Observer). This research has made use of the NASA/IPAC Extragalactic Database, which is operated by the Jet Propulsion Laboratory, California Institute of Technology, under contract with the National Aeronautics and Space Administration.

REFERENCES

Altieri, B. 2003, MOS Optical Loading (XMM-SOC-CAL-TN-0043 Issue 1.1; Noordwijk: ESA)
Bechtold, J., et al. 2003, ApJ, 588, 119
Becker, R. H., White, R. L., & Helfand, D. J. 1995, ApJ, 450, 559
Begelman, M. C. 1978, MNRAS, 185, 847
———. 2002, ApJ, 568, L97
Bernardi, M., et al. 2003, AJ, 125, 1849
Binney, J., & Merrifield, M. 1998, Galactic Astronomy (Princeton: Princeton Univ. Press)
Boller, Th., Tanaka, Y., Fabian, A. C., Brandt, W. N., Gallo, L., Anabuki, N., Haba, Y., & Vaughan, S. 2003, MNRAS, 343, L89
Boroson, T. A., & Green, R. F. 1992, ApJS, 80, 109
Brandt, W. N., Laor, A., & Wills, B. J. 2000, ApJ, 528, 637
Burrows, D., et al. 2005, Space Sci. Rev., 120, 165
Chen, X., Abramowicz, M. A., Lasota, J.-P., Narayan, R., & Yi, I. 1995, ApJ, 443, L61
Choi, J., Leighly, K. M., & Matsumoto, C. 2005, BAAS, 37, 447
Collin, S., & Kawaguchi, T. 2004, A&A, 426, 797

Djorgovski, S., & Davis, M. 1987, ApJ, 313, 59
Dunlop, J. S. 2004, in Coevolution of Black Holes and Galaxies, ed. L. C. Ho (Cambridge: Cambridge Univ. Press), 341
Dunlop, J. S., McLure, R. J., Kukula, M. J., Baum, S. A., O'Dea, C. P., & Hughes, D. H. 2003, MNRAS, 340, 1095
Elvis, M., et al. 1994, ApJS, 95, 1
Ferrarese, L., & Merritt, D. 2000, ApJ, 539, L9
Frank, J., King, A., & Raine, D. 1992, Accretion Power in Astrophysics (2nd ed.; Cambridge: Cambridge Univ. Press)
Gallagher, S. C., Brandt, W. N., Chartas, G., & Garmire, G. P. 2002, ApJ, 567, 37
Gallo, L. C. 2006, MNRAS, 368, 479
Gallo, L. C., Boller, T., Brandt, W. N., Fabian, A. C., & Grupe, D. 2004a, MNRAS, 352, 744
Gallo, L. C., Tanaka, Y., Boller, Th., Fabian, A. C., Vaughan, S., & Brandt, W. N. 2004b, MNRAS, 353, 1064
Gebhardt, K., et al. 2000, ApJ, 543, L5
Gehrels, N., et al. 2004, ApJ, 611, 1005
Green, P. J., Aldcroft, T. L., Mathur, S., Wilkes, B. J., & Elvis, M. 2001, ApJ, 558, 109
Grupe, D., & Mathur, S. 2004, ApJ, 606, L41
Grupe, D., Thomas, H.-C., & Leighly, K. M. 2001, A&A, 369, 450
Haro, G., & Luyten, W. J. 1962, Bol. Inst. Tonantzintla, 3, 37
Jenkins, E. B., Bowen, D. V., Tripp, T. M., & Sembach, K. R. 2005, ApJ, 623, 767
Jenkins, E. B., Bowen, D. V., Tripp, T. M., Sembach, K. R., Leighly, K. M., Halpern, J. P., & Lauroesch, J. T. 2003, AJ, 125, 2824
Kato, S., Fukue, J., & Mineshige, S. 1998, Black-Hole Accretion Disks (Kyoto: Kyoto Univ. Press)
Kawaguchi, T., Shimura, T., & Mineshige, S. 2001, ApJ, 546, 966
Koratkar, A., & Blaes, O. 1999, PASP, 111, 1
Kubota, A., & Done, C. 2004, MNRAS, 353, 980
Laor, A. 2000, NewA Rev., 44, 503
Laor, A., & Netzer, H. 1989, MNRAS, 238, 897
Leighly, K. M. 1999a, ApJS, 125, 297
———. 1999b, ApJS, 125, 317
———. 2001, in X-Ray Emission from Accretion onto Black Holes, ed. T. Yaqoob & J. H. Krolik (Baltimore: Johns Hopkins Univ.), in press
Leighly, K. M., Halpern, J. P., Helfand, D. J., Becker, R. H., & Impey, C. D. 2001, AJ, 121, 2889
Leighly, K. M., Halpern, J. P., & Jenkins, E. B. 2004, in ASP Conf. Ser. 311, AGN Physics with the Sloan Digital Sky Survey, ed. G. T. Richards & P. B. Hall (San Francisco: ASP), 277
Leighly, K. M., Halpern, J. P., Jenkins, E. B., & Casebeer, D. A. 2007, ApJS, in press (Paper II)
Leighly, K. M., & Moore, J. R. 2004, ApJ, 611, 107
Leighly, K. M., Zdziarski, A. A., Kawaguchi, T., & Matsumoto, C. 2002, in X-Ray Spectroscopy of AGNs with *Chandra* and *XMM-Newton*, ed. Th. Boller et al. (MPE Rep. 279; MPE: Garching), 259
Loewenstein, M., & White, R. E., III. 1999, ApJ, 518, 50
Magorrian, J., et al. 1998, AJ, 115, 2285
Martel, A. R., et al. 2003, AJ, 125, 2964
Mason, K. O., et al. 2001, A&A, 365, L36
Mathur, S., & Grupe, D. 2005, ApJ, 633, 688
Matsumoto, C., Leighly, K. M., & Kawaguchi, T. 2004, Prog. Theor. Phys. Suppl., 155, 377
McLure, R. J., & Dunlop, J. S. 2002, MNRAS, 331, 795
Miniutti, G., & Fabian, A. C. 2004, MNRAS, 349, 1435
Onken, C. A., Ferrarese, L., Merritt, D., Peterson, B. M., Pogge, R. W., Vestergaard, M., & Wandel, A. 2004, ApJ, 615, 645
Page, K. L., O'Brien, P. T., Reeves, J. N., & Breeveld, A. A. 2003, MNRAS, 340, 1052
Peterson, B. M., & Wandel, A. 2000, ApJ, 540, L13
Peterson, B. M., et al. 2004, ApJ, 613, 682
Porquet, D., Reeves, J. N., O'Brien, P., & Brinkmann, W. 2004, A&A, 422, 85
Pounds, K. A., Done, C., & Osborne, J. P. 1995, MNRAS, 277, L5
Prescott, K. 2006, M.S. thesis, Univ. Oklahoma
Proga, D. 2005, ApJ, 630, L9
Roming, P. W. A., et al. 2005, Space Sci. Rev., 120, 95
Ryan, C. J., De Robertis, M. M., Virani, S., Laor, A., & Dawson, P. C. 2007, ApJ, 654, 799
Shimura, T., & Takahara, F. 1993, ApJ, 419, 78
———. 1995, ApJ, 440, 610
Smith, M. J. S. 2004, PN Optical Loading (XMM-SOC-CAL-TN-0051 Issue 1.1; Noordwijk: ESA)
Steffen, A. T., Strateva, I., Brandt, W. N., Alexander, D. M., Koekemoer, A. M., Lehmer, B. D., Schneider, D. P., & Vignali, C. 2006, AJ, 131, 2826
Strateva, I. V., Brandt, W. N., Schneider, D. P., Vanden Berk, D. G., & Vignali, C. 2005, AJ, 130, 387
Strüder, L., et al. 2001, A&A, 365, L18
Stuhlinger, M., et al. 2006, Status of *XMM-Newton* Instruments Cross-Calibration with SAS, ver. 6.5 (XMM-SOC-CAL-TN-0052 Issue 3.0; Noordwijk: ESA)
Svensson, R., & Zdziarski, A. A. 1994, ApJ, 436, 599
Tanaka, Y., Boller, Th., Gallo, L., Keil, R., & Ueda, Y. 2004, PASJ, 56, L9
Turner, M. J. L., et al. 2001, A&A, 365, L27
Vaughan, S., Boller, Th., Fabian, A. C., Ballantyne, D. R., Brandt, W. N., & Trümper, J. 2002, MNRAS, 337, 247
Wandel, A., & Boller, T. 1998, A&A, 331, 884
White, R. L., Becker, R. H., Helfand, D. J., & Gregg, M. D. 1997, ApJ, 475, 479
Wilkes, B. J., Tananbaum, H., Worrall, D. M., Avni, Y., Oey, M. S., & Flanagan, J. 1994, ApJS, 92, 53
Vestergaard, M., & Peterson, B. P. 2006, ApJ, 641, 689
Zdziarski, A. A., & Gierlinski, M. 2004, Prog. Theor. Phys. Suppl., 155, 99